

10. Infrared Radiation of Planetary Nebulae

10.1 The Structure of the Infrared Spectrum

The emission lines of gaseous nebula with wavelengths from 1 μm up to 100 μm are attributed to the infrared band. The corresponding composition and typical structure of the PN spectra is shown in Fig. 10.1.

It is convenient to divide this range into the following three intervals:

Near infrared	1–5	μm
Mid infrared	5–30	μm
Far infrared	30–100	μm

The strongest in the near infrared is the well known line of neutral helium 10830 \AA = 1.083 μm HeI; usually it is as intense as the H_β line of hydrogen. With the line 1.083 μm HeI is blended the third line of the Paschen series of hydrogen, 1.09 P_γ , though it is fainter by an order of magnitude. Then comes the weak line 2.17 μm Br_γ of the Brackett series, and the rather faint line 3.74 μm $\text{P}f_\gamma$ of the Pfund series.

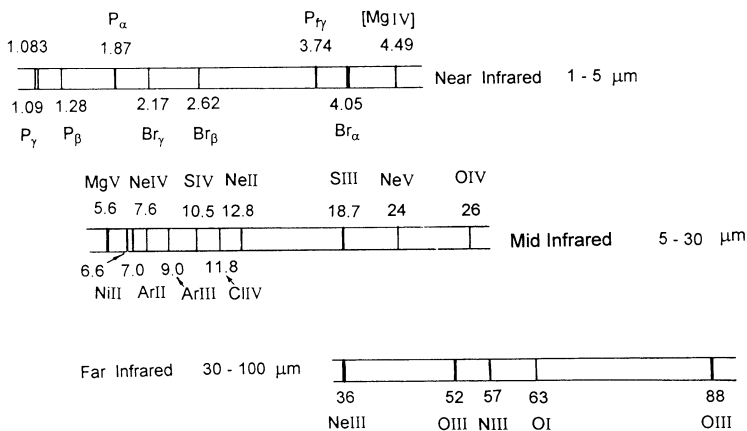


Fig. 10.1. Composition and general structure of the infrared spectrum of gaseous nebulae in the region of wavelengths 1–100 μm . Conditional limits of different parts: near infrared – 1–5 μm ; mid-infrared – 5–30 μm ; far infrared – 30–100 μm . All lines in the mid- and far infrared are forbidden

The middle infrared is quite rich, 5–30 μm , band. Here the strongest structure consists of two lines: 10.52 [SIV] and 15.56 [NeIII], of nearly the same intensities compared with the strength of the H_β line. In certain nebulae these forbidden lines are even stronger – 2–4 times – than the H_β line (e.g. NGC 7009, NGC 6153, NGC 7354). These lines are detected for practically for all PNs. The cases when the infrared spectrum of the nebula is given only by a single pair of lines, 10.5 [SIV] and 15.6 [NeIII], are common.

Next are the lines 9.0 [ArIII] and 18.7 [SIII]. The faintest in the mid infrared are the lines 12.8 [NeIII] and 14.3 [NeV], by an order weaker than the mentioned lines, 10.5 [SIV] and 15.6 [NeV].

The most exotic infrared line of five-fold ionized neon 7.65 [NeVI] has been also discovered (e.g. in the high excitation class PN NGC 6302 ($p = 1$)).

The far infrared, 30–100 μm , is represented by two forbidden lines, the doublet 52 [OIII] and 88 [OIII], arising at the transitions between sublevels of the ion O^{++} . The line 52 [OIII] is weaker in absolute intensity than the line 5007 [OIII] by three (NGC 3242, NGC 6543, NGC 6826) up to ten times (NGC 2440) (Pottasch et al., 1986). The critical electron concentration for these lines is relatively small: $\sim 6 \times 10^3 \text{ cm}^{-3}$ for 52 [OIII] and $\sim 7 \times 10^2 \text{ cm}^{-3}$ for 88 [OIII], and therefore in many PNs these lines would be strongly suppressed. This is the reason for the weakness and even the absence of these lines in the spectra of dense PNs (NGC 7027).

Both the infrared forbidden lines, 52 [OIII] and 88 [OIII], were observed in 1981 in the spectra of PNs of various excitation classes (NGC 6543, NGC 6720 etc.) as well as in diffuse nebulae (M 17, W 43, W 49 etc.) (Watson et al., 1981). The infrared line of doubly ionized nitrogen, 57.3 [NIII], also exotic, has been detected in the spectra of diffuse nebulae (M 17, W 43).

10.2 Infrared Emission Lines of Nebulae

The presence of four categories of infrared emission lines should be expected in the spectrum of planetary and diffuse nebulae: (a) recombination lines of hydrogen and helium; (b) forbidden lines of different ions; (c) molecular bands of hydrogen and other elements; (d) Molecular emission bands of dust component of nebula – heated crystals and dust particles.

Let us illustrate the situation with the example of the PN NGC 7027, which has been studied in great detail. This nebula has been observed in the ranges 0.9–2.7 μm , 2–4 μm , 2–14 μm , 8–13 μm . Observations have indicated the following:

(a) Emission lines of hydrogen of the following series:

Paschen	($i \rightarrow 3$):	1.87 P_α , 1.28 P_β , 1.09 P_γ ,
Brackett	($i \rightarrow 4$):	4.05 Br_α , 2.62 Br_β , 2.17 Br_γ up to 1.53 Br_{19} ,
Pfund	($i \rightarrow 5$):	3.74 Pf_α .

- (b) Rather faint emission lines of molecular hydrogen (H_2): 2.42 μm , 2.41 μm , 2.12 μm .
- (c) Faint emission lines of neutral helium : 1.083 HeI, 2.06 HeI, as well as one or two lines of ionized helium: 1.01 HeII(4–5).
- (d) Forbidden lines 1.04 [NI], 1.03 [SII], 0.95 [SIII], 0.91 [SIII].

Intensities $F(\lambda)$ of the strongest among these lines corrected for interstellar extinction are given in Table 10.1.

Over a hundred emission lines in the region 0.68–1.05 μm have also detected in the spectrum of NGC 7027 (Pequignot, Baluteau, 1988). Among the identified ones were the recombination lines of hydrogen HI in the Paschen series (up to the line $n = 40$), of ionized helium HeII in the series (5, n) and (6, n) (up to line $n = 43$) and neutral helium HeI of few series ($3l, nl$). In all cases the observed intensities fit the predictions of photoionization theory, perfectly.

Estimation of theoretical intensities of infrared forbidden lines do not represent any difficulty if the numerical values of the atomic parameters are known. In fact, there are only two: the Einstein coefficients of spontaneous transitions A_{ij} and the “collision strength” $\Omega(ij)$. Corresponding calculations for a large number of infrared forbidden lines have been performed by Petrosian (1970), as well as by Simpson (1975). Results for most interesting ions and configurations p and p^5 as well as p^2 and p^4 (doublets) are given in Table 10.2.

Historically, the first infrared line of three times ionized sulphur 10.5 [SIV] was simultaneously detected in the early 1970s in the spectra of three PNs – NGC 7027, NGC 6572 and NGC 7009.

The second infrared line, 9.0 [ArIII], was detected in NGC 7027 and NGC 6572, with intensities two orders smaller than the calculated ones.

The third line, 12.8 [NeII], was observed in five PNs, NGC 7027, 7662, 6572, IC 418 and BD+30°3639. Along with [SIV], [ArIII] and [NeII] other infrared lines were also observed in the spectrum of NGC 7027, e.g. at 3.09, 3.3, 11.3, 11.4 μm , etc. Obviously, these first airborne observations were continued with tremendous intensity by space missions.

Table 10.1. Observed intensities, $F(\lambda)/F(\text{H}\beta)$, of the most intense infrared emission lines in the spectrum of the planetary nebula NGC 7027. $F(\text{H}\beta) = 21.9 \times 10^{-10}$ ergs $\text{cm}^{-2}\text{s}^{-1}$

Line [λ , μm]	$F(\lambda)/F(\text{H}\beta)$	Line [λ , μm]	$F(\lambda)/F(\text{H}\beta)$
1.083 HeI	0.854	2.17 Br $_{\gamma}$ (7–4)	0.038
0.95 [SIII]	0.492	3.74 Pf $_{\gamma}$ (8–5)	0.007
1.28 P $_{\beta}$ (5–3)	0.112	0.4686 H $_{\beta}$	1
1.09 P $_{\gamma}$ (6–3)	0.069		

Table 10.2. Calculated intensities $F(\lambda)$ of a number of infrared forbidden lines of some ions in units of $F(10.5 \text{ [SIV]}) = 100$

Line, λ , μm	$F(\lambda)$	Line, λ , μm	$F(\lambda)$
Configuration p		Configuration p^5	
10.53 [SIV]	100	12.79 [NeII]	40
25.87 [OIV]	10	3.21 [CaICV]	0.7
34.8 [SiII]	2	6.98 [ArII]	0.3
Configuration p^2		Configuration p^4	
88.16 [OIII]	3.9	147 [OI]	0.06
51.69 [OIII]	14.9	63.07 [OI]	0.7
24.15 [NeV]	1.0	35.20 [NeIII]	0.9
14.32 [NeV]	0.7	15.35 [NeIII]	10
33.65 [SIII]	17	21.84 [ArIII]	0.2
18.68 [SIII]	21	9.00 [ArIII]	3

Do the *infrared emission lines* have a crucial role by virtue of their informativeness and significance for the physics of PNs? It can seem strange but the answer to this question seems to be negative. Infrared emission lines can provide us mainly with information on three parameters: the electron temperature T_e (not always), electron concentration n_e and relative abundance of a given ion, N_i/N_p , while we have already learned how to successfully determine these parameters with the help of forbidden lines in the visual, and now also in ultraviolet region.

The infrared observations of the *continuous* spectra of nebulae nevertheless have led to a discovery of exceptional importance, i.e. of the *dust particles as permanent components of PNs*.

In spite of this remarkable fact, the observations in *infrared lines* can hardly have fundamental consequences for the physics of gaseous nebulae.

10.3 IRAS: Infrared Spectra of Planetary Nebulae

Observations of all infrared lines presenting astrophysical interest turn out to be possible only if the infrared telescope is located outside the Earth's atmosphere.

The first intense infrared observations of PNs in space conditions were connected with the launching in 1983 on a polar orbit of a special astrophysical satellite *IRAS* – the *InfraRed Astronomical Satellite*, with the infrared telescope on board equipped with a cryogenic system. The observations have been carried out in four bands centred at 12, 25, 60 and 100 μm .

The first list of *IRAS* observations already contains the data on the radiation fluxes of 64 PNs in the following lines (Pottasch et al., 1986):

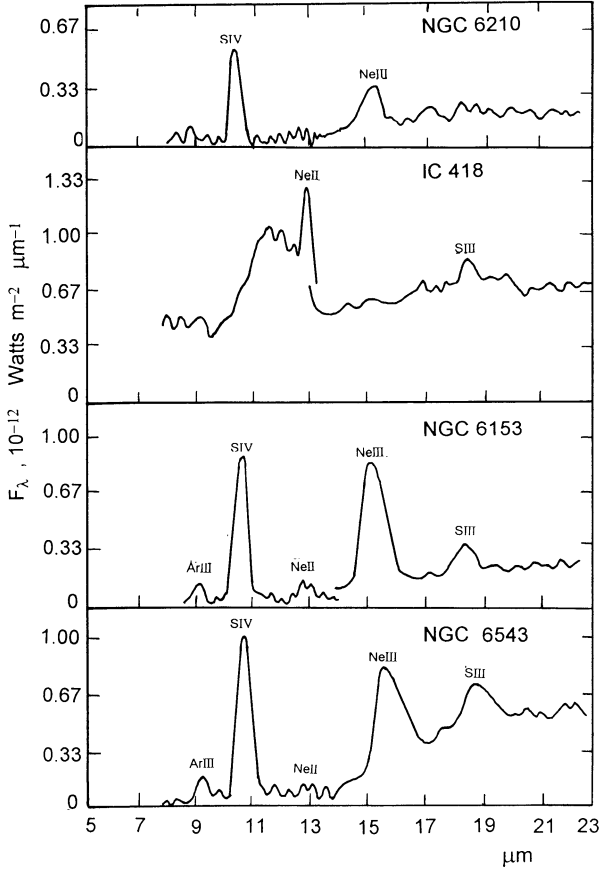


Fig. 10.2. *IRAS* recordings of the infrared spectra for four planetary nebulae in the wavelength region of 7–23 μm . The strongest lines are indicated

7.65 [NeVI]	10.52 [SIV]	14.3 [NeV]	18.7 [SIII]
9.0 [ArIII]	12.8 [NeII]	15.56 [NeIII]	

IRAS recordings of infrared spectra in the region of 7–23 μm for four PNs are shown in Fig. 10.2. Certain features are common to all these spectra; they contain both components – the continuous spectrum and emission lines. The behaviour of the continuous spectrum is not the same, however. In some cases it falls quickly starting from $\sim 14 \mu\text{m}$ and even disappears at $\sim 10 \mu\text{m}$ (NGC 6210, NGC 6153) at the level of flux sensitivity of $\sim 3 \times 10^{-14} \text{ W m}^{-2} \mu\text{m}^{-1}$. For other objects, on the other hand, the level of the continuous spectra varies weakly (IC 418). The composition of lines seems more stable: the forbidden lines of ArIII, SIII, SIV, NeII, NeIII are typically fixed.

In some nebulae, (NGC 6153 and NGC 6543), the line 15.5 [NeIII] is the strongest, the first component of the doublet [NeIII]. The second component

Table 10.3. Results of *IRAS* observations of the infrared emission line 15.5 μm [NeIII] in the spectrum of four planetary nebulae

Planetary nebula	p	$F(\text{H}\beta)$ [$10^{-14}\text{W}\text{s}^{-1}$]	$\frac{F(15.5)}{F(\text{H}\beta)}$	$\frac{F(3\ 686)}{F(15.5)}$	$T_e(155)$ [K]	$T_e([\text{OIII}])$ [K]
NGC 6 153	6	15	4.7	0.20	7 200	8 400
NGC 6 210	4	10	1.3	0.60	9 000	9 570
NGC 6 543	5	28	2.5	0.20	7 200	8 230
IC 418	1	50	0	—	—	8 420

of this doublet, 35.2 [NeIII], in accordance with calculations, must be weaker by an order of magnitude, i.e. below the *IRAS* working sensitivity. Note that in many PNs the line 15.5 [NeIII] is stronger than $\text{H}\beta$ (Table 10.3).

The next line, by its strength, is 10.52 [SIV] (p). The line of moderate strength 18.7 [SIII], the first component of the doublet [SIII] (p^2), is visible in almost all nebulae. The second component, 33.6 [SIII], nearly of the same strength, again was out of the working range of the telescope. The remaining lines, 8.99 [ArIII] and 12.82 [NeII], are rather weak and at the limit of discovery.

Besides these lines, a rather powerful emission band was fixed at 11.3 μm in the spectrum of IC 418 and Cn 1–1, both of low excitation classes. Clearly, the excitation of this band is connected with dust particles.

The line 15.5 [NeIII] is more sensitive with respect to the electron temperature T_e than to the electron concentration n_e . For example, the ratio of intensities $F(3\ 869\ \text{\AA}\ [\text{NeIII}])/F(15.5\ \mu\text{m}\ [\text{NeIII}])$ depends weakly on n_e , and therefore can be used as an indicator for the determination of T_e . This dependence is given in Fig. 10.3 (see Pottasch, 1984). Using the data of ground based observations of the line 3 869 [NeIII] (Pottasch et al., 1986), the values of $T_e = T_e(15.5)$ were estimated by known values of the ratio of $F(3\ 868)/F(15.5)$ (fifth column of Table 10.3) for a sample of four low excitation (p) PNs. The results are given in the sixth column of Table 10.3. In the last column the values of $T_e = T_e([\text{OIII}])$, obtained using the “[OIII] method” i.e. with the help of the ratio $N_1 + N_2/4\ 363$ (Table 6.1), are given. In all three cases the accordance between both T_e is quite good; hence, the electron temperatures obtained are related to one and the same region.

To summarize, we may conclude that space observations in the infrared emission line of PNs in the range 7–2/3 μm do not lead to extraordinary conclusions nor to the necessity of revising existing viewpoints on the composition of PNs.

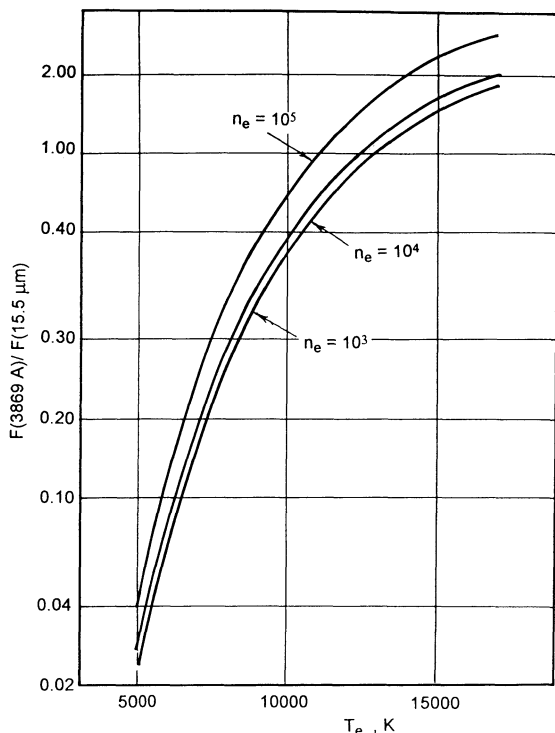


Fig. 10.3. The theoretical dependence between the electron temperature of nebulae T_e and the ratio of the intensities of the lines 3896 \AA [NeIII] and $15.5 \mu\text{m}$ [NeIII], for three values of the electron concentration n_e : 10^5 , 10^4 and 10^3 cm^{-3}

10.4 The Nature of Infrared Emission of Planetary Nebulae

From the energy point of view, the observed infrared emission of PNs in the region of $1\text{--}30 \mu\text{m}$ occurs almost completely in continuous emission; the contribution of infrared emission lines is small – of the order of 5–10%. The absolute flux of infrared emission is much larger compared with the continuum of all atoms and ions as well as thermal bremsstrahlung.

From here, the first important conclusion can be drawn: *infrared continuous emission of PNs cannot be of atomic origin.*

The spectrum of infrared emission as a rule becomes stronger towards the long wavelength region. Usually the maximum of the spectrum occurs at $10\text{--}30 \mu\text{m}$, which corresponds to a black-body temperature of $300\text{--}100 \text{ K}$, i.e. two orders smaller than the nebula's electron temperatures.

Hence, the second important conclusion is: *infrared emission of PNs is not determined by the high electron temperature of nebulae.*

Obviously at such low temperatures, $100\text{--}300 \text{ K}$, gas in the nebula cannot radiate. Hence, the observed infrared emission should be related to the

thermal emission of the dust particles within the nebula. The heating can be performed in any way – either by absorption of powerful ultraviolet radiation of the central star, or the no less powerful L_α radiation of the nebula itself, or by collisions with the high energy particles, such as electrons, proton beams, etc. At the same time, heating up to a temperature of 100–300 K, clearly, does not result in the evaporation of crystals themselves.

Thus, the third important conclusion is: *the dust particles or the crystals of solid matter are, together with the hot gas – plasma – the permanent component of PNs.*

The idea of the existence of dust particles in PNs goes back to the 1960s, when quite unexpectedly powerful infrared emission was discovered in NGC 7027 (Gillet et al., 1967), and the impossibility of its generation by free-free emission was demonstrated (Delmar et al., 1967).

The continuous spectrum in the region $\lambda > 2.9 \mu\text{m}$ is much higher (by two orders of flux magnitude) than the extrapolated level of radio emission (free-free continuum). This additional emission is attributed to the thermal emission of dust particles.

According to direct measurements, the absolute flux of infrared emission is of the order and even larger than the L_α flux of nebulae. This makes it highly probable that the assumption on the heating of dust particles in nebulae via the absorption of L_α photons is correct. Meanwhile, in optically thick nebulae 75% of L_c energy transforms to L_α energy (Chap. 11); hence, the flux of L_α radiation in nebulae really must be very high. The possibility of heating of dust particles by L_α radiation was noticed just after the discovery of infrared emission in NGC 7027 in 1967.

Hence, the fourth important conclusion is: *the heating of dust particles in nebulae is realized via the hydrogen ionizing energy emitted by the central star of the nebula.*

There are no theoretical reasons excluding the existence of dust particles in strongly heated gaseous media. The collisions of dust particles with thermal ions or electrons at the kinetic temperatures $\sim 10\,000$ K is not connected with any destruction effects either for the crystals (silicates, carbonates etc.) or dust particles (see Sect. 10.6).

However, the conclusions that the infrared emission is issued by the heated dust particles and that the heating of dust particles is realized by L_α photons have to be checked quantitatively.

10.5 Parameters of Dust Particles

Consider the question of the determination of the parameters of dust particles in the nebula by the data from infrared observations.

Let N be the number of L_α photons appearing in an ionized zone per unit time and per unit volume. Obviously this rate must be equal to that of the recombinations of free electrons with protons: $n_1 = n_e n^+ \alpha_r = n_\alpha^2 \alpha_r$,

where α_r is effective coefficient of recombination on levels $n > 2$. The total luminosity in L_α photons of the nebula with a volume V will be

$$L_\alpha = n_e^2 \alpha_r h\nu_\alpha V, \quad (1)$$

where $h\nu_\alpha$ is the energy of an L_α photon.

Let q be the fraction of L_α energy spent on heating dust particles within the nebula. According to the conjecture made above, the energy qL_α absorbed by dust particles is reemitted in the infrared range. Therefore we can write for the infrared luminosity L_{IR}

$$L_{\text{IR}} = qn_e^2 \alpha_r h\nu_\alpha V. \quad (2)$$

Assuming the same mean mass for all PNs,

$$n_e V = \text{const}, \quad (3)$$

we have from (2)

$$L_{\text{IR}} \sim n_e. \quad (4)$$

This is a remarkable relationship indicating a linear correlation between the infrared luminosity and the electron concentration in the nebula, if we adopt the “dust” nature of infrared radiation and the heating of dust particles by L_α radiation.

The results of homogeneous infrared observations by Cohen and Barlow (1974) for a sample of PNs and in the wavelength interval 2.2–22 μm , which are still of importance, are given in Table 10.4. As an immediate result one has T_{IR} , the effective temperature obtained by the Planckian fit of the observed distribution of energy, and L_{IR} , the absolute infrared luminosity obtained according to the expression

$$L_{\text{IR}} = 4\pi D^2 F_{\text{IR}}, \quad (5)$$

where D is the distance of the nebula and F_{IR} is the observed IR flux.

The infrared energy emitted by a particle of radius a by the black-body temperature will be $4\pi a^2 \sigma T_{\text{IR}}^4 Q_i$, where σ is the Stefan–Boltzmann constant and Q_i is the efficiency of emission by particle in infrared. The total number of particles is $n_d V$, where n_d is the particle concentration. Therefore we have for the total infrared luminosity of the nebula

$$L_{\text{IR}} = 4\pi \alpha^2 \sigma T^4 Q_i n_d V. \quad (6)$$

Equating this expression with (2), we obtain

$$T = n_e^{1/2} \left(\frac{q\alpha_r h\nu_\alpha}{4\pi n_d a^2 Q_i \sigma} \right)^{1/4} \sim n_e^{1/2}, \quad (7)$$

i.e. the “infrared” temperature of the nebula T_{IR} must vary, depending on the electron concentration, relatively slowly, according to $\sim n_e^{1/2}$.

Table 10.4. Infrared effective temperatures T_{IR} and infrared luminosity L_{IR} for a sample of planetary nebulae

Planetary nebula	T_{IR} [K]	n_e [10^3cm^{-3}]	$\frac{L_{\text{IR}}}{L_{\odot}}$	$\frac{L_{\text{IR}}}{L_{\odot}}$
NGC 2 440	185	3.27	105	0.4
NGC 6 210	175	2.43	1 000	3.8
NGC 6 302	185	5.53	520	2.5
NGC 6 439	–	1.38	520	2.8
NGC 6 543	–	7.60	130	2.7
NGC 6 572	174	8.42	4 900	4.5
NGC 6 741	205	12	700	0.5
NGC 6 751	170	0.7	480	5.5
NGC 6 790	245	37.3	14 600	3.2
NGC 6 803	190	4.16	1 100	2.0
NGC 6 807	185	13	3 800	2.3
NGC 6 826	–	2.3	123	0.2
NGC 6 881	200	11.2	1 700	1.2
NGC 6 884	210	6.62	410	0.5
NGC 6 886	165	9.85	1 400	1.1
NGC 6 891	–	1.66	40	0.3
NGC 6 905	–	0.53	22	0.5
NGC 7 009	350	4.73	210	0.6
NGC 7 026	200	6.15	710	2.0
NGC 7 027	210	25.5	11 400	3.6
NGC 7 662	–	3.06	23	0.08
IC 418	250	14.1	950	0.5
IC 2 149	170	6.36	390	0.7
IC 2 165	190	7.68	500	0.5
IC 3 568	–	4.57	24	0.1
IC 4 593	155	2.2	155	1.7
IC 4 634	155	3.14	300	1.7
IC 4 997	175	18.2	15 000	6.5
IC 5 117	205	30.4	11 400	3.0
IC 5 217	–	7.0	250	0.3
A 30	155	0.035	255	7.8
A 78	135	0.024	300	4.6
BD+30°3639	210	15.2	25 500	13
Cn 3–1	155	8.56	2 600	2.3
Hu 1–2	–	5.88	130	0.2
Hu 2–1	200	12.9	3 100	1.9

The values of T_{IR} and L_{IR}/L_{\odot} , obtained in this manner are given in the second and third columns of Table 10.4. In the fourth column, the values of n_e are collected from different sources. First, note that neither the law $L_{\text{IR}} \sim n_e$, nor $L_{\text{IR}} \sim n_e^{5/2}$ fit the data, and, second, the dependence $T_e \sim n_e^{1/2}$ again is far from satisfactory.

We have for the complete mass of dust particles \mathcal{M}_{\odot}

$$\mathcal{M}_d = n_d V \rho_d \frac{4\pi}{3} a^3. \quad (8)$$

Comparing this with (6) we obtain

$$\mathcal{M}_d = \rho_d \frac{a}{3Q_i} \frac{L_{\text{IR}}}{\sigma T_{\text{IR}}^4}, \quad (9)$$

where r_d is the density of the dust particle.

Using the numerical values of constants and bearing in mind that $Q_i = 2\pi a/\lambda_m$, where λ_m is the wavelength of the maximum on the IR spectral curve of the nebula, we obtain at $\lambda_m \approx 20 \mu\text{m}$ and $r_d \approx 3 \text{ g cm}^{-3}$

$$\frac{\mathcal{M}_d}{\mathcal{M}_{\odot}} = 9.21 T_{\text{IR}}^{-4} \frac{L_{\text{IR}}}{L_{\odot}}. \quad (10)$$

The scatter in values of T_{IR} of PN included in Table 10.4 is not large, on average $T_{\text{IR}} \sim 200 \text{ K}$, while the scatter in the magnitudes of L_{IR}/L_{\odot} is large. Therefore, we have from (10)

$$\frac{\mathcal{M}_d}{\mathcal{M}_{\odot}} = 5.8 \times 10^{-9} \frac{L_{\text{IR}}}{L_{\odot}}. \quad (11)$$

The limiting values of the ratio L_{IR}/L_{\odot} vary from 20 (NGC 7662, NGC 6826) to 2.5×10^4 (BD+30°3639). The limiting values of \mathcal{M}_d should be in the range $(10^{-7}-10^{-4})\mathcal{M}_{\odot}$, respectively.

Adopting for the mass of purely gaseous nebula $\mathcal{M}_g \approx 0.1\mathcal{M}_{\odot}$, we then have

$$\frac{\mathcal{M}_d}{\mathcal{M}_g} \sim 10^{-6} - 10^{-3}.$$

For the interstellar medium the ratio $\mathcal{M}_d/\mathcal{M}_g$ is of the order $10^{-3}-10^{-2}$. This discrepancy is real, and in all cases PNs cannot be considered as suppliers of dust to interstellar medium.

10.6 Heating of Dust Particles in Nebulae

In the last column of Table 10.4, the ratios of infrared luminosity, L_{IR} , to the Lyman alpha luminosity, L_α , are given. The latter, L_α , is obtained from the observed radio emission S_ν on the frequency ν , generated by thermal electrons at free-free transitions and on the assumption that total number of ionized photons L_c , emitted by the central star, is equal to the total number of L_α photons, emitted by the nebula (Chap. 11). The following relationship for the L_α luminosity of nebula was derived by Rubin in 1968:

$$L_{L_\alpha} = L_c h\nu_\alpha = 7.77 \times 10^{54} \nu_\alpha^{0.1} S_\nu T_e^{-0.45} D^2 \text{ ergs s}^{-1}. \quad (12)$$

From (5) and (11) we have

$$\frac{L_{\text{IR}}}{L_{L_\alpha}} = 4.68 \times 10^{-56} T_e^{0.45} \frac{F_{\text{IR}}}{S_\nu}, \quad (13)$$

i.e. the ratio $L_{\text{IR}}/L_{L_\alpha}$ is independent of the nebula's distance and therefore acquires the status of an independent parameter.

In accordance with to the conjecture of the heating of dust particles by L_α radiation, one must expect the condition: $L_{\text{IR}}/L_\alpha < 1$ to be fulfilled. Meanwhile, judging by the data in Table 10.4, for the majority of nebulae ($\sim 60\%$), $L_{\text{IR}}/L_{L_\alpha} > 1$, in certain cases even being about 10.

Clearly the L_α radiation cannot be the only source of heating of dust particles in PNs.

A way out of this situation may be the assumption that the heating of dust particles is realized under the action of direct L_c radiation of the central star, part of which is the L_α radiation of the nebula. Note that only those L_c photons are transformed into L_α -photons which are located near the limiting frequency $\nu_0 n$ (912 \AA), while at high frequencies this efficiency falls sharply, according to $\sim \nu^{-3}$. Thus, the efficiency of absorption of a photon by hydrogen falls to half at $\lambda \sim 725 \text{ \AA}$, being only 10% at $\lambda \sim 425 \text{ \AA}$ and 1% at $\lambda \sim 200 \text{ \AA}$. One can therefore assume that the wavelength region shorter than 500 \AA remains practically unused by hydrogen and, hence, cannot be transformed into L_α -photons. In other words, of the total ultraviolet energy E_u , emitted by the central star, only a small fraction E_c is used by the nebula and transformed into L_α photons. This unused resource of energy $E_c(E_u/E_c - 1)$ can lead to the direct heating of dust, without transforming into L_α photons.

Obviously, this resource of ultraviolet energy, E_u/E_c , is equal

$$\frac{E_u}{E_c} = \frac{1}{1 - e^{-\tau_c}} \frac{\int_{x_0}^{\infty} \frac{x^3 dx}{e^x - 1}}{x_0^3 \int_{x_0}^{\infty} \frac{dx}{e^x - 1}}, \quad (14)$$

where $x_0 = h\nu_0/kT_* = 159\,000/T_*$, and the term $(1 - e^{-\tau_c})$ takes into account that the nebula can be optically thin ($\tau_c < 1$) at frequencies of hydrogen ionization.

Clearly the “resource factor”, E_u/E_c , can be identified with L_{IR}/L_α . As the calculations indicate, even at $T_* \sim 30\,000$ K and $\tau_c \gg 1$, this factor is more than unity, of the order of 10 at $\tau_c \sim 0.2$. This resource is quite large, of the order of 10 and larger for PN with high temperature nuclei, $T_* \sim 60\,000$ K and higher.

The question, to what extent this resource of ultraviolet energy is used and absorbed by the dust particles needs separate examination. There are reasons to assume that the efficiency of absorption of ultraviolet photons by dust particles should be higher than that of the L_α photons.

Thus, our conjecture made above and its consequences on the heating of dust particles by L_α radiation can be generalized in the form of a *fifth main conclusion*: the heating of dust particles in nebulae is realized mainly by radiation of the central star in the far ultraviolet, shorter than 500 Å.

10.7 The Morphology of the Dust Component of a Nebula

The comparison of infrared maps of individual nebulae with their optical images leads to the following conclusions by their morphological character:

- (a) In some cases (NGC 7027, BD+30°3639) the infrared images of different wavelength are in mutual correlation and even correlate with the images in hydrogen lines (Bentley et al., 1984).
- (b) The phenomenon of bipolarity of the nebula in certain cases is evident in both bands – in dust emission and in the emission of gas.
- (c) For some objects (NGC 6302) the infrared morphology is in marked discrepancy with that in optical band (Lester, Dinerstein, 1984).

Thus, in general, one cannot exclude the possibility of “morphological surprises” on the basis of infrared observations. On this occasion, the detailed consideration of the influence of the genuine magnetic field of nebulae on the distribution of dust particles is of particular interest (see Chap. 17).

10.8 Infrared Lines of [OIII]

The thin structure of the ground state 3P of the ion O^{++} includes three sublevels, 3P_0 , 3P_1 and P_2^3 : transitions between them lead to the forbidden infrared lines, 52 μm [OIII] and 88 μm [OIII] (Fig. 10.4). These lines are associated with the known forbidden lines N_1 (5007 Å) and N_2 (4959 Å)

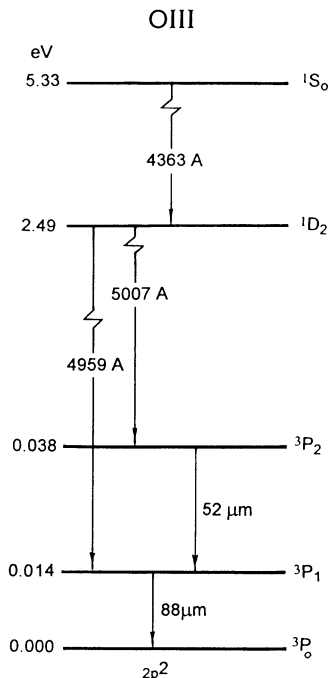


Fig. 10.4. Energy levels of [OIII]

appearing at the transitions from the upper level 1D_2 to 3P_2 and 3P_1 , respectively.

The intensities of the lines 52 [OIII] and 88 [OIII] do not depend on the electron temperature T_e but do depend on the electron concentration n_e . However, the intensities of the lines N_1 and N_2 both depend on T_e and n_e .

All these lines are excited by electron collisions, and the ratio of intensities, e.g. of the line N_1 to the intensity of the line 52 [OIII], must depend on both T_e and n_e . In this connection the following question arises: can one gain by

Table 10.5. Observed fluxes $F(\lambda)$, in units of 10^{-10} ergs $\text{cm}^{-2} \text{s}^{-1}$, in forbidden lines of [OIII], 52 μm , 88 μm and 5 007 Å, and values of n_e (in 10^3 cm^{-3}) and T_e , obtained with the help of these lines for four planetary nebulae

Planetary nebula	$F\lambda$			n_e, cm^{-3}		T_e, K	
	52	88	5 007	52/88	[OII]	5 007/52	[OIII]
NGC 2 440	1.72	0.48	19.4	1.6	1.6	13 000	14 300
NGC 3 242	4.41	1.63	19.2	1.0	2.0	9 800	11 500
NGC 6 543	8.79	1.10	27.0	10	4	5 800	8 000
NGC 6 826	3.66	0.96	9.2	1.6	1.6	7 700	8 800

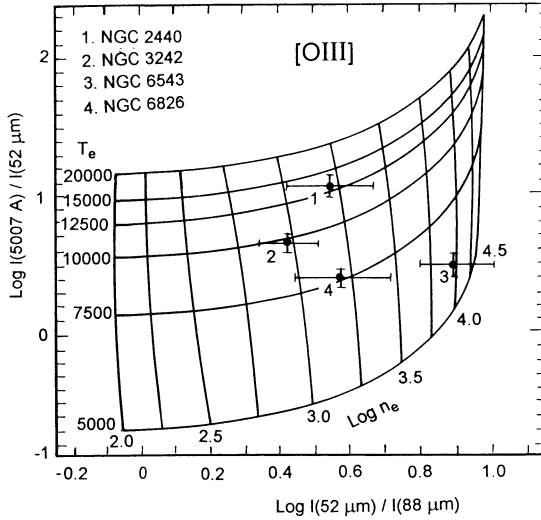


Fig. 10.5. Dependence between the intensities of lines of [OIII], in the infrared, 52 and 88 μm , and the optical, 5007 \AA , as calculated for various values of n_e and T_e . The locations of four planetary nebulae are shown: 1 – NGC 2440, 2 – NGC 3242, 3 – NGC 6543, 4 – NGC 6826

combined observations in the optical lines of N_1 and N_2 , and in the infrared ones of 52 [OIII] and 88 [OIII] for the physics of PNs?

Ground based observations of the lines 52 [OIII] and 88 [OIII] are impossible, but can be performed, say, in airborne conditions. In Table 10.5 the results of measurements by a 91 cm infrared airborne telescope (Dinerstein et al., 1985) of the 52 [OIII] and 88 [OIII] line fluxes for a sample of PNs are presented, along with the fluxes in line 5007 [OIII]. Using the known atomic parameters for these lines, the computed curves of dependence between the ratios of the fluxes $F(52)/F(88)$ and $F(5007)/F(52)$ were constructed for various values of n_e and T_e (Fig. 10.5).

Using the observed values of the ratios $F(52)/F(88)$ and $F(5007)/F(52)$, we can obtain n_e and T_e . The results are presented in Table 10.5 along with the values of n_e and T_e obtained earlier by means of traditional methods, i.e. based on the forbidden doublet 3726 [OII]/3729 [OII] (for n_e) and $N_1 + N_2/4363$ [OIII] (for T_e).

From these results the following conclusions can be drawn:

- Electron concentrations obtained using the infrared lines [OIII] almost coincide with those derived from the optical lines of [OIII].
- Electron temperatures obtained with the help of the infrared lines [OIII] are systematically lower than the temperatures obtained by the optical lines of [OIII]. The discrepancy between these “infrared” and “optical” temperatures is too large – 1000–2000 K – and has a systematic character.

The second conclusion is of special importance, since once more it confirms that nebulae are non-isothermal systems and seem to possess a separate zone of infrared emission.

10.9 The Temperature of Dust in Planetary Nebulae

Obviously, one of the remarkable features of PNs, the identity of electron temperatures for all PNs, should be considered. It varies within quite narrow limits with respect to the mean value, 10 000 K, for PN with enormous scattering in the main physical parameters, including the diversity of temperatures of their central stars.

What is the situation with the dust temperature in the nebula? The results of infrared observations carried out in the range of 3–108 μm (Moseley, 1980) combined with the observations mentioned above (Table 10.4), enable one to construct the infrared spectra in the wavelength range from 2.2 μm up to 108 μm . These spectra obtained, with two or three exceptions, have common features for all PNs: a clearly expressed maximum near 30 μm corresponding to a black-body temperature of ~ 100 K, i.e. what was discovered earlier for NGC 7 027 (Fig. 14.11).

Thus, the mean temperature of the dust is also a kind of a universal parameter for all PNs, analogous to the electron temperature of the gas.

The sample of PNs in Table 10.4 includes objects of various ages, very young, such as IC 4 997, 150 years old, and rather old, and as A 30, 20 000 years old; in both cases the infrared temperatures are practically the same. One can conclude that the dust particles do not undergo essential evolution of *physical* and *optical* properties during the evolution of the nebula itself. If so, then the dust particles in the nebula must be of primordial origin.

10.10 The Survival of Dust Particles in Nebulae

Dust particles cannot be formed in a purely gaseous medium of the nebula by a kind of atomic collision, even if the gas density is rather large – for this the nebula is too hot.

Infrared observations confirm the presence of dust–gas envelopes surrounding many cool giants and supergiants and, hence, the very process of formation of dust particles within the dense cool atmospheres, in principle, is possible.

So, dust particles do exist primordially in the outer parts of stellar atmospheres, far away from stars, i.e. in kinds of surrounding and presumably expanding envelopes. One can think that at a definite stage of its expansion this envelope can evolve to what we call a *planetary nebula* – an ionized medium with a temperature of 10 000 K, under the action of short wavelength radiation.

In this connection the crucial problem is that of the survival of dust particles under the influence of intense central radiation.

The elementary act which can destroy the dust particle is the tearing off of electrons from its surface under the action of ultraviolet radiation, i.e. the “photon alienation” of electrons. As a result, the positively charged dust particle starts to merge with either free electrons or positive ions, finally becoming either more positive or negative.

In conditions of stationarity the following three processes can occur: (a) the photon alienation of an electron from the dust particle under the central ultraviolet radiation; (b) the impact or capture of an electron by dust particles; (c) the impact or capture of a proton by dust particles.

The solution of the corresponding differential equations describing these processes reveals the evolution of dust particle properties with time. The preliminary conclusions are as follows:

- (a) In central parts of the nebula the photon tearing processes dominates, and the dust particles have to be charged positively.
- (b) In the outer parts of the nebula the impacts of electrons with dust particles dominate, and particles have to be charged negatively.
- (c) The charge of dust particles should be very high: $Z \approx +400$ in the central parts of the nebula and $Z \approx -400$ in the outer ones.

In the latter case the electrostatic force on the particle’s surface should: $Ze^2/a \approx 0.005Z \approx 2$ eV, which coincides with the tearing off energy of atoms from the particles’ surface (≈ 2 eV), as well as with the photon mean energy within the nebula.

Thus, the destruction of dust particles seems to be possible. The question is how efficient this process can be, i.e. how fast a particle can vanish. Rough estimation yields for the duration of the dust particle’s life $t_{\text{in}} \approx 10^{15}a/N_p$ year in central regions of nebula and $t_{\text{out}} \approx 3 \times 10^{12}a/N_p$ in outer ones. Adopting $a \sim 3 \times 10^{-5}$ cm and $N_p \approx 10^{-3}$ cm⁻³ for their concentration, we obtain $T_{\text{in}} \approx 10^7$ year and $t_{\text{out}} \approx 10^5$ year. This result seems to be paradoxical, so far as it predicts that particles live in central parts of a nebula longer than in its periphery. However, in both cases the lifetime of the dust particles exceeds the lifetime of the PN itself, i.e. 100 000 years.

10.11 Infrared Lines and the Temperatures of Nuclei

The presence of emission lines of FeVII, NV, NeV or NeVI in the spectrum of a PN is an obvious indication of a very high temperature of its nucleus – higher than 100 000 K. Ions of higher degrees of ionization, however, rarely give emission lines in optical and even ultraviolet regions convenient for registration.

In certain cases the presence of highly ionized ions can be established by emission lines emitted by these ions also in the infrared region. Such an

example was mentioned above (Sect. 3) and was related to the line 7.65 [NeVI] – five-times ionized neon; it is detected in the spectrum of high excitation nebulae (NGC 6302) ($p = 10$). Ionization potentials of NeV and NeVI are equal to 126 eV and 158 eV, which correspond to nuclear radiation in the region shorter than 100 Å and 80 Å.

There are two more infrared forbidden lines, 1.96 [SiVI] and 2.48 [SiVII], belonging to five and six times ionized silicon, both simultaneously resonances, with the ionization potentials of 167 eV and 205 eV. These lines enable one to penetrate too far – up in to 74 Å and 60 Å in the nucleus spectra. These lines were also observed in PN spectra (NGC 6302 and NGC 6537) (Ashley, Hyland, 1988).

The ratio of intensities of the lines 1.96 [SiVI] and 2.48 [SiVII] depends on the nucleus temperature T_* . The corresponding relationship may be derived by applying the condition of detailed ionization equilibrium. As a result, $T_* \approx 430\,000$ K for NGC 6302 and $T_* \approx 240\,000$ K for NGC 6572 have been obtained.

Thus, the infrared lines of [SiVI] and [SiVII] can be used successfully as powerful indicators of the PN nuclei of superhigh temperatures. From this point of view the importance of these kind of infrared observations is obvious.

10.12 Evolution of Dust Particles in Planetary Nebulae

Do the main parameters of dust particles – the effective temperature T_d , sizes a , their total mass in nebula \mathcal{M}_d , their total number N_p , the ratio of mass of both dust and gas components, $\mathcal{M}_d/\mathcal{M}_g$ etc. – remain constant during the lifetime of a PN? The importance of this question is unquestionable for our understanding of the evolution of PN themselves.

This problem was considered by Lenzuni and collaborators (1989) for a sample of 233 PNs observed by *IRAS*. Their methods were basically those described in Sect. 5. Note that the expansion velocity does not depend on the linear sizes of nebulae, therefore one can consider the dependence of parameters only on the nebula radius R_n .

The main results are as follows:

- (a) The sizes of the dust particle decreases with the increase of the nebula's radius R_n according to:

$$a \propto R_n^{-1.86}, \quad (15)$$

as is shown in Fig. 10.6(a). The points denote the *IRAS* data, i.e. the fluxes in bands 25, 60 and 100 μm ; circles denote data only in bands 25 and 60 μm .

The limiting values of dust particle sizes are: from 4×10^{-5} cm at $R_n = 10^{16}$ cm up to 3×10^{-8} cm at $R_n = 10^{18}$ cm. This means that with the aging of nebulae, the dust particles become smaller while bigger particles dominate in young, new-born nebulae.

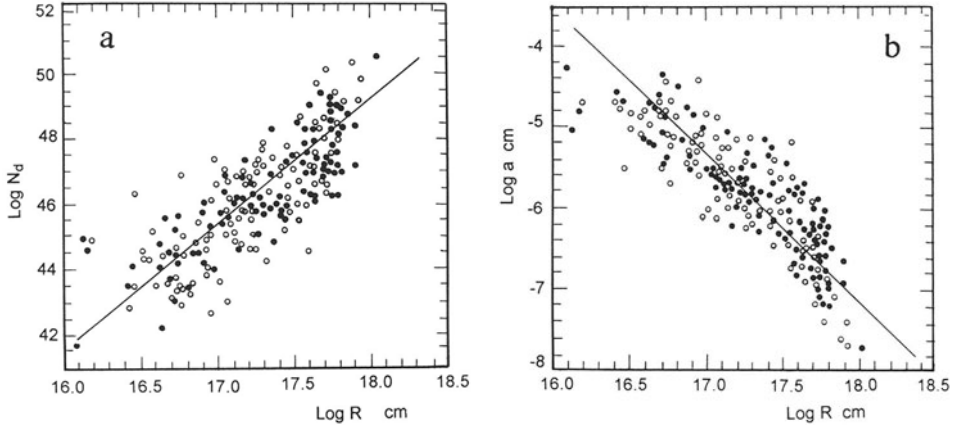


Fig. 10.6. (a) Graphical dependence between the sizes of dust particles a and the radius of the nebula R_n according to *IRAS* data for 233 PNs. Dots denote observations in the bands of 25, 60 and 100 μm ; circles, those only in the bands of 25 and 60 μm . (b) The same as in (a) but for the dependence between the total number of dust particles N_d and R_n

- (b) The total number of dust particles N_d increases rapidly in accordance with the law

$$N_d \propto R_n^{+4.19}, \quad (16)$$

as is shown in Fig. 10.6(b). The limiting values of $N_d \sim 10^{42}$ at the birth of a nebulae up to $\sim 10^{50}$ particles at the end of its life – the scatter yields eight (!) orders of magnitude. The crucial role of decaying processes is obvious.

- (c) The total mass of dust in the nebula \mathcal{M}_d decreases according to the law

$$\mathcal{M}_d \propto R_n^{-1.66}, \quad (17)$$

however, with strong scattering of observational points. On average, $\mathcal{M}_d \sim 3 \times 10^{-4} \mathcal{M}_\odot$ at $R_n \sim 2.5 \times 10^{17}$ cm. The limiting magnitudes are from $\sim 10^{-2} \mathcal{M}_\odot$ at the moment of formation of the nebula, and up to $10^{-5} \mathcal{M}_\odot$ at the end of its life. The sweeping-up of dust particles from the nebula is obvious.

- (c) The effective temperature of dust particles T_d statistically is less sensitive, in accordance with the conclusion drawn in Sect. 10.5, to the nebula's size

$$T_d \propto R_n^{-0.4}. \quad (18)$$

The limiting values of T_d differ slightly as well: only three times, from 50 K up to 150 K.

- (d) The ratio of the mass of both dust and gas components, $\mathcal{M}_d/\mathcal{M}_g$ varies in wide limits – from 0.2 in young nebulae up to 10^{-4} in old ones. On average $\mathcal{M}_d/\mathcal{M}_g \sim 0.001$. This is at least two orders larger than the values mentioned in Sect. 10.5.

- (e) The optical depth of dust particles at the frequencies of the Lyman continuum t_α was obtained as well: they were within limits from 0.005 up to 1–2, on average 0.1, however, without noticeable signs of evolution.
- (f) The limiting values of infrared luminosities of PN L_{IR}/L_\odot , bolometric luminosity of nucleus L_{bol}/L_\odot in the case of the mentioned selection of 233 PNs are as follows:

L_{IR}/L_\odot :	min	5	NGC 6 853, IC 1 295, A 20
	max	7 800	NGC 7 027
L_{bol}/L_\odot :	min	300	NGC 5 315, NGC 1 501, Hu 1–2
	max	14 400	NGC 7 027
$L_{\text{IR}}/L_{\text{bol}}$:	min	0.2	NGC 6 853, H 2–41
	max	70	M 2–9

Of special importance from the point of view of the theory of heating of dust particles is the ratio $L_{\text{IR}}/L_{\text{bol}}$. For a sample of 36 PNs (Table 10.4), this ratio is larger than unity for 60% of objects. For the sample of 233 PN this ratio turns out to be larger than unity in 80% (!) of cases. For six nebulae this ratio is even larger than 10. Thus, now we have another impressive indication that the L_α radiation of nebulae cannot be the only source of heating of dust particles. A decisive role here should be played by heating by the direct radiation of the central star in the far ultraviolet, at wavelengths shorter than 500 Å, as was outlined above, in Sect. 10.6.

Moreover, judging by the fact that in certain cases the ratio $L_{\text{IR}}/L_{\text{bol}}$ is larger than 0.8, i.e. quite near to unity, one can conclude that in those PNs (M 2–9, M 1–26, He 2–108 etc.) the heating of dust particles under the action of the stellar wind or the fast electrons from the central star should have a dominant role.

The discrepancy in the values of the main parameters of dust particles in both samples, with 36 and 233 objects, is of a systematic nature; in the latter ($N = 233$) the values of T_d are on 1.5–2 times smaller than we have in the first case, while just T_d plays crucial role in computations of the remaining parameters. Nevertheless, it is difficult to doubt the correctness of the main conclusion: all or almost all the parameters of the dust particles undergo evolutionary variations.

Thus, the dust particles in PNs continuously undergo processes of decay, erosion and sweeping out under the actions, presumably of corpuscular beams of nuclei, stellar wind and hard ultraviolet radiation.

The reasons for variations and the details of evolutionary parameters of dust particles in PNs, as well as the role of numerous other effects, such as “particle–particle” collisions, the final stages of the evaporation of dust particles, are a matter for special study.